

Resonant Modes in Parallel Josephson Junction Arrays for Submm Oscillator Applications

F. Boussaha, J-G. Caputo, C. Chaumont, A. Féret, and T. Vacelet

Abstract—We report on the development of submm oscillators using parallel Josephson junctions unevenly distributed within a superconducting stripline. To optimize their RF operation within a desired bandwidth, a straightforward method has been used. The radiation emitted from the arrays is detected using integrated SIS twin-junctions. Despite the small junction number ($N=21$), the I - V characteristics of the detector exhibit clearly photon-assisted quasiparticle steps when the array is biased upon Josephson resonances ranging from 370 to 500GHz. The array has a moderate current density of $\sim 6\text{kA/cm}^2$ and provides an output power around $0.28\mu\text{W}$ which is sufficient to achieve sensitive integrated heterodyne receivers. Furthermore, the parallel array approach can also be extended to higher frequencies using high critical temperature superconducting materials.

I. INTRODUCTION

Parallel SIS array concept has already been theoretically and experimentally investigated with the aim of implementing tunable oscillators [1-4]. However, most studies were done by considering only arrays without taking into account some important engineering aspects related, for example, to the power coupling towards an external circuit (antenna, RF coupler), expected frequencies of operation, bandwidth of interest, etc. Indeed, the typical studied arrays feature an identical distance between two adjacent junctions which is likely randomly set. To achieve efficient and usable oscillators, we designed, fabricated and characterized parallel arrays comprising a few small Nb/AlO_x/Nb-based SIS junctions ($N=21$) [5] which are parallel-connected to a superconducting Nb/SiO/Nb microstrip line. The array is capacitively coupled, through an RF/DC block, to a sub-mm SIS-based detector to detect the emitted radiations. Using the electrical model of fig.1, the array is optimized as a RLC circuit where $R=R_j$ is the quasiparticle current, $L=L_j$ is the Josephson inductance and $C=C_j$ the intrinsic capacitance junction. This lead to an irregular distribution of junctions within a superconducting Nb/SiO/Nb microstrip line. As a first order, we linearized the Josephson nonlinear admittance produced by the Josephson current $I=I_c \sin(\varphi)$ where φ is the phase difference of the two superconductor electrodes by a constant inductance $L_j = \Phi_0 / 2\pi I_c$ where $I_c = J_c S_{j_array}$ is the critical current of the SIS junction. In this paper, we experimentally study the different Josephson modes of the array that optimized as an oscillator in 320-600GHz band.

II. CIRCUIT AND EXPERIMENTAL RESULTS

Figure 2 presents the 21-junction array coupled to a SIS-based detector through a slotline/microstrip transition which acts as a

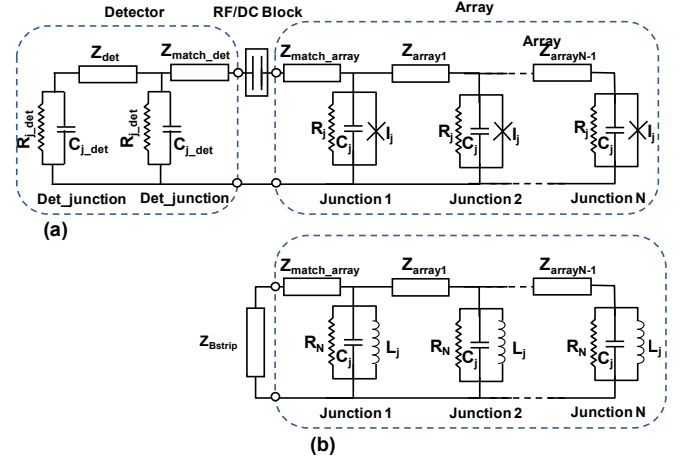


Fig. 1. (a) Equivalent model of the circuit consisting of a SIS junction array capacitively coupled to a SIS-based detector through a RF/DC block. Each SIS junction is modeled by its intrinsic capacitance C_j , quasiparticles conductance $G_j = I/R_j$ and Josephson current $I_j = I_c \sin(\varphi)$ in parallel. (b) The Josephson nonlinear admittance is linearized by a constant inductance $L_j = \Phi_0 / 2\pi I_c$ and quasiparticle resistance R_j is taken close to the normal resistance R_N .

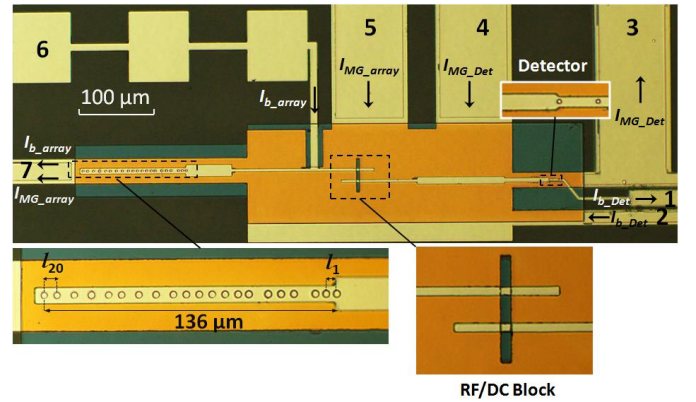


Fig. 2. Photograph of the typical optimized parallel array-based circuit which consists of: twin Nb/AlO_x/Nb SIS junction detector, dc-block made and parallel arrays of 21 Nb/AlO_x/Nb junctions. $I_{1,20} = 5, 5, 10, 6, 6, 9, 5, 6, 6, 6, 6, 8, 8, 8, 6, 8, 8, 8, 6\mu\text{A}$.

RF/DC block. Further details can be found in [5]. Fig. 3-a shows the I - V curve of the array which displays resonances right before jumping to the voltage gap (not shown in the figure), for different values of the applied magnetic field generated by a current I_{MG_array} passing through a control line. I_{MG_array} ranges from 85 to 174mA. For clarity, the measured resonance voltages are converted in frequencies using $f_{res} = V_{res} / \Phi_0$.

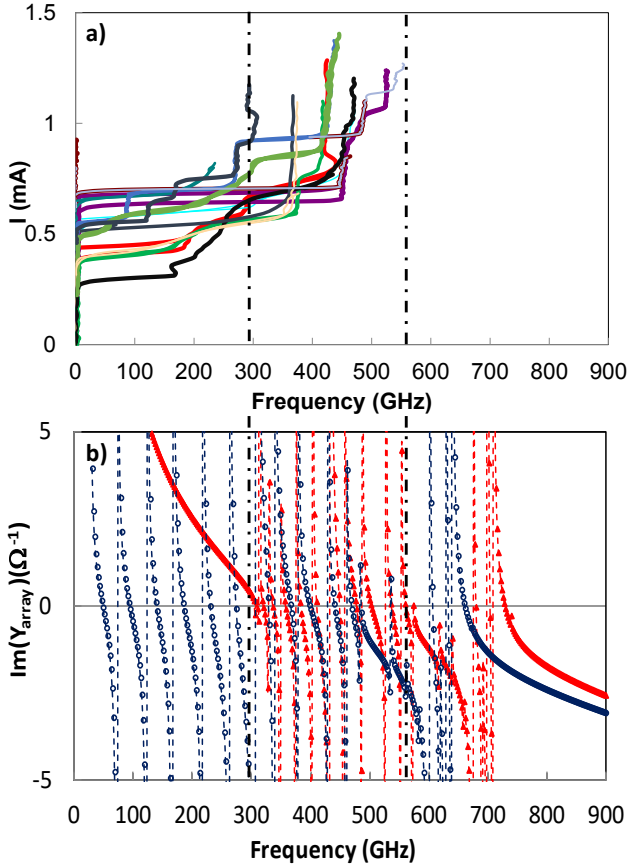


Fig. 3. Array's I - V curve showing resonances excited by magnetic fields generated by currents I_{MG_array} ranging from 85 to 174mA. The array admittance $Y_{array}(\omega)$ includes the linearized Josephson admittances $(J_L \omega)^{-1}$. To compare with the simulated imaginary $\text{Im}[Y_{array}(\omega)]$ (curve below), the voltages of resonances are converted in frequencies using $V_{res} \times 483.59 \text{GHz}$.

Depending on the current magnitude, we can distinguish 2 resonant modes. The first mode occurs up to ~ 266 GHz and shows up six steps featuring low current magnitude, between $V_{res}=0.1$ and $0.55 \pm 0.01 \text{mV}$. In frequency, this leads to $f_{res}=V_{res}/\Phi_0=48$ GHz and $266 \pm 4.83 \text{GHz}$, respectively. The resonances appear with nearly regular voltage step of $\Delta V_{res}=0.08 \pm 0.01 \text{mV}$ ($\Delta f_{res}=38 \pm 4.83 \text{GHz}$) at the same voltage locations whatever the magnetic field strength. The second resonant mode displays sharp resonances with significantly higher current magnitude occurring from $V_{res}=0.55$ to $1.14 \pm 0.01 \text{mV}$. This yields $f_{res}=V_{res}/\Phi_0 \approx 266$ to 551GHz which corresponds to the optimized bandwidth limits [5]. Unlike the first mode, there are not equidistant in voltage and their respective voltage position depends strongly upon I_{MG_array} values (i.e., magnetic field). In order to access the resonant frequencies, we plot the imaginary part of the array admittance $Y_{array}(\omega)$ as function of the frequency. Thus, the resonances occurred when $\text{Im}[Y_{array}(\omega)]$ goes to 0 [6]. The blue curve (circle) shows the $\text{Im}[Y_{array}(\omega)]$ in the absence of the Josephson inductive element while the red curve (triangle) shows the $\text{Im}[Y_{array}(\omega)]$ when it is taken into account. Further detailed analysis of both modes will be reported elsewhere. To access whether output powers come out of the array, we exited

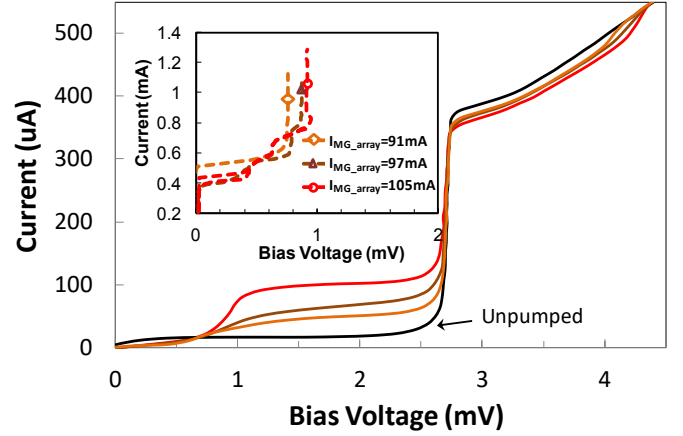


Fig. 4. Measured detector's I - V characteristics pumped at 381, 411, 440GHz when the 21-junction array is tuned at $V_{res}=0.79, 0.85, 0.91 \text{mV}$ respectively. The inset shows the resonances obtained for $I_{MG_array}=91, 97$ and 105mA , respectively. The measured unpumped curve is obtained when the array is biased out of the resonance at $V_{bias}=0$ or $V_{bias}>V_{res}$.

resonances whose frequencies are expected within the detector bandwidth. The radiation emitted from the arrays is detected using the integrated SIS twin-junctions. The I - V characteristics of the detector clearly exhibit photon-assisted quasiparticle steps when the array is biased upon its Josephson resonances ranging from 370 to 500GHz. Figure 4 displays the detector's I - V curve when the array is biased at $V_{res}=0.79, 0.85$ and $0.91 \pm 0.01 \text{mV}$. These correspond to emitted frequencies $f_{res}=V_{res}/\Phi_0=381, 411, 440 \pm 4.83 \text{GHz}$, respectively. The resonances are excited with magnetic fields generated by currents $I_{MG}=91, 97$ and 105mA , respectively. The unpumped curves are obtained when arrays are biased out of resonances either at $V_{bias}=0$ or at $V_{bias}>V_{gap}$. From the I - V pumped curve, the calculation of frequencies using the photon-assisted steps $f_{ph}=e(V_{gap}-V_{ph})/h$ gives same frequencies than the emitted ones. The maximum pumping is reached at $440 \pm 4.83 \text{GHz}$ with $V_{res}=0.91 \pm 0.01 \text{mV}$ and $I_{MG}=105 \text{mA}$. The array has a moderate current density ($J_c \approx 6 \text{kA/cm}^2$) and provided an output power around $0.28 \mu\text{W}$ which would be sufficient to achieve sensitive heterodyne reception [5].

REFERENCES

- [1] A. V. Ustinov, M. Cirillo, B. H. Larsen, V. A. Oboznov, P. Carelli, and G. Rotoli, "Experimental and numerical study of dynamic regimes in a discrete sine-Gordon lattice", Phys. Rev. B 51, 308, 1995.
- [2] H.S.J. Van der Zant, E.H. Vischer, D. R. Curd, T.P. Orlando, "Vortex dynamics in one-dimensional parallel arrays of underdamped Josephson junctions," IEEE Trans. On Appl. Superconductivity, Vol. 3, No. 1, 1993.
- [3] Y. M. Zhang and P. H. Wu, "Numerical calculation of the height of velocity-matching step of flux-flow type Josephson oscillator," J. Appl. Physics 68, 4703, 1990.
- [4] S. Han, B. Bi, W. Zhang, and J. E. Lukens, "Demonstration of Josephson effect submillimeter wave sources with increased power," Appl. Phys. Lett. 64, 1424, 1994.
- [5] F. Boussaha, C. Chaumont, A. F eret, J-G. Caputo and T. Vacelet "Optimized Non-Uniform Nb SIS parallel Josephson junction array oscillators", IEEE Transactions on Applied Superconductivity, Vol. 26, Issue 3, 2016.
- [6] M. Salez and F. Boussaha, "Fluxon modes and phase-locking at 600 GHz in superconducting tunnel junction nonuniform arrays," J. Appl. Phys. 107 (013908), (2010).